Article

Chemical Transformation of Lignosulfonates to Lignosulfonamides with Improved Thermal Characteristics

Karolina Komisarz *[ID], Tomasz M. Majka [ID] and Krzysztof Pielichowski [ID]

Department of Chemistry and Technology of Polymers, Faculty of Chemical Engineering and Technology, Cracow University of Technology, ul. Warszawska 24, 31-155 Kraków, Poland; tomasz.majka@pk.edu.pl (T.M.M.); kpielich@pk.edu.pl (K.P.)
* Correspondence: karolina.komisarz@doktorant.pk.edu.pl

Abstract: Lignin is an abundantly occurring aromatic biopolymer that receives increasing attention as, e.g., a biofiller in polymer composites. Though its structure depends on the plant source, it is a valuable component showing biodegradability, antioxidant, and ultra-violet (UV) absorption properties. Lignosulfonates, a by-product of the paper and pulping industries formed as a result of the implementation of the sulfite process, have been used in the presented study as a raw material to obtain a sulfonamide derivative of lignin. Hereby, a two-step modification procedure is described. The obtained materials were investigated by means of FTIR, WAXD, SS-NMR, SEM, and TGA; the results of spectroscopic investigations confirm the formation of a sulfonamide derivative of lignin via the proposed modification method. The obtained modified lignin materials showed significantly improved thermal stability in comparison with the raw material. The internal structure of the lignosulfonate was not altered during the modification process, with only slight changes of the morphology, as confirmed by the WAXD and SEM analyses. The manufactured sulfonamide lignin derivatives show great promise in the potential application as an antibacterial filler in advanced biopolymeric composites.

Keywords: biocomposites; biopolymers; chemical modification; lignosulfonate; sulfonamides

1. Introduction

Lignin is a naturally occurring, branched aromatic polymer, co-existing in plant organisms with cellulose and hemicelluloses, and, due to its abundance, it is the most common macromolecule comprised of the aromatic moieties [1–3]. Although cellulose and hemicelluloses are classified as polysaccharides, the structure of lignin comes from the combination of the three phenylpropane-based structures, stemming from precursor compounds known as monolignols—p-coumaryl, coniferyl, and sinapyl alcohols (Figure 1) [4]. The content of the structures originating from each monolignol varies between the sources of lignin acquisition and directly impacts the composition and properties of the resultant material [5–7]. The dependency of the lignin structure on the source of acquisition, as well as the difficulties with the repeatability of its properties, hinders the potential application possibilities. Currently, only 5% of lignin is explored in low-value uses or used as a resource for energy production and recovery [8]; however, there is a growing interest in its application as a renewable source of aromatic hydrocarbons [7,9,10]. For many years, lignin was primarily considered a waste, but its potential was taken into consideration as early as the 1950s, when Nord and Schubert pointed out the fact that this massive source of aromatic hydrocarbons is wasted away because of the limited ways to obtain chemically pure lignin, as such extracted only in a time-consuming process utilizing fungi enzymes (the so-called 'brown rot' fungi, capable of digesting cellulose). Other industrially used methods of lignin extraction, such as sulfite or Kraft processes, were somehow destructive and yielded products containing impurities from the used chemicals. The extraction using alcohols is also possible; however, it only yields a fraction of the lignin from a plant source, namely, the alcohol-soluble constituents [7,11].
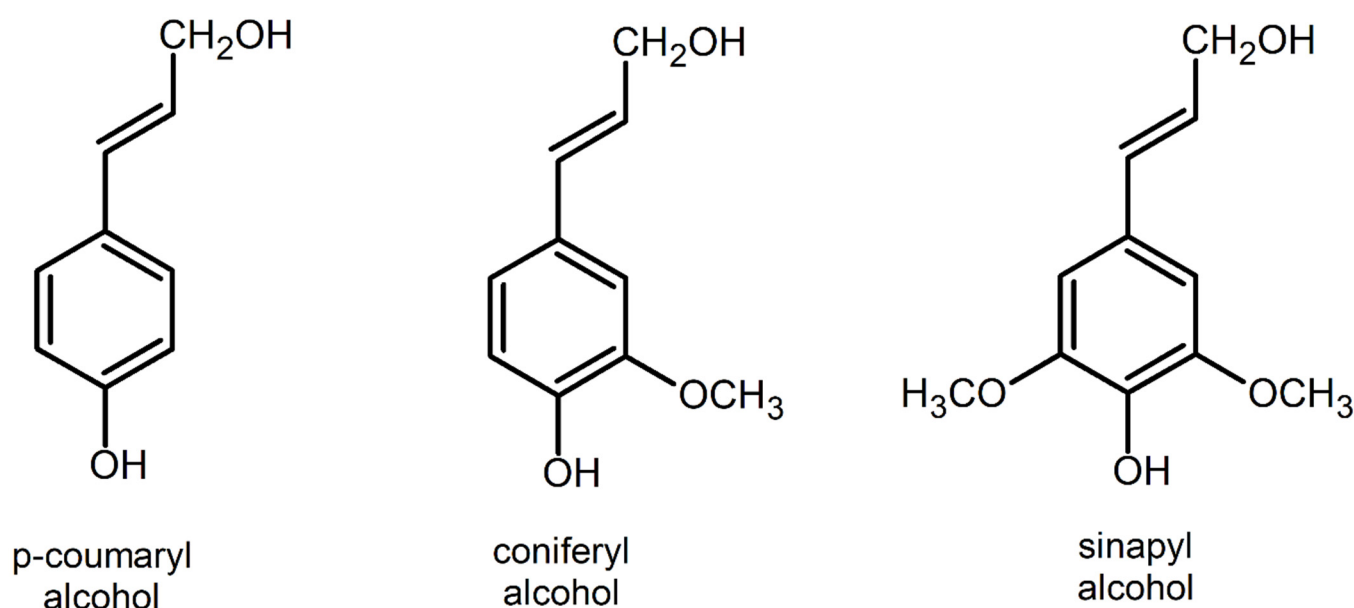
Figure 1. Monolignols-precursor molecules responsible for the intrinsic structure of lignin.

There are four known methodologies used for the extraction of lignin from the lignocellulosic biomass. Two grades of technical lignins—Kraft lignin and lignosulfonates, collectively known as sulfur lignins—are obtained as a by-product in the paper and pulping industry in the processes requiring the sulfur-based compounds. Lignosulfonates are obtained in the sulfite process [12], where lignocellulosic biomass is boiled with the aqueous solution of sulfur dioxide, and with the addition of the suitable hydroxide (ammonium, calcium, magnesium, or sodium) [8], the corresponding metal sulfites are formed. In the next step, sulfite ions present in the solution are introduced into the lignin structure, yielding benzyl sulfonic acid units [12]. The resultant product, a lignosulfonate, is water-soluble due to the presence of polar sulfonic groups, and its sulfur content varies between 4 and 8 percent [13]. The choice of the base used in the process affects the chemical reactivity of the lignosulfonates towards further modifications—ammonium lignosulfonate has the highest reactivity, whereby calcium-based compounds are the least active [14,15]. Lignosulfonates also show promise in catalytic studies as catalyst carriers [16].

Although unmodified lignin displays many attractive features, such as biodegradability, good thermal stability, antioxidant properties, and the ability to absorb UV-rays [17,18], applying chemical modification procedures allow for obtaining lignin-based materials with enhanced properties via utilization of various types of reactions, such as esterification [19], etherification [20,21], epoxidation [22], and amination [23], to name a few [24]. Other methods to obtain value-added chemicals employ depolymerization of lignin to simple molecules and then their use as building blocks in the synthesis of the new functional materials [25].

Recently, in a study by Jiang et al., lignin-derived-nano-biochar was introduced into the styrene–butadiene rubber. The obtained material was proposed as an alternative to commercial carbon black and provided significant improvement of the tensile properties and vulcanization rate of the composites. The overall reinforcing effect of the lignin-derived char filler was comparable with that of commercial carbon black [26]. Additionally, research concentrating on utilizing dihydroxybenzophenone-grafted lignin with high UV absorbance was described, and the obtained product showed great promise as an alternative for commercial sunscreens [27]. The intrinsic absorption abilities of lignin were further enhanced by either introduction of the calcium counter-ions [28] or grafting with poly (acrylic acid) [29]. Such-prepared materials proved effective in scavenging the cationic dyes from the dyestuff effluents [28] and show great promise in the selective absorption of ofloxacin and ciprofloxacin [29]. Current studies also investigate the usage of the lignin-based prod-

uct as wood adhesives for medium-density fiberboards [30] or functional hydrogels with conductive properties, with the potential to use them as a sunscreen or even flexible electronic skin [31]. The aforementioned studies show a great interest in utilizing lignin and its derivatives and exploring their potential as alternatives for many commercial products.

In the presented work, a different approach to lignin modification is described. The sulfonyl groups present in the aromatic network of lignosulfonates are subjected to a two-step modification procedure to yield a sulfonamide derivative of lignin: first, to obtain lignosulfonyl chloride by means of a reaction of lignosulfonate with chlorosulfonic acid, and second, to obtain lignin sulfonamide by a reaction with a secondary amine. Patent literature describes a similar approach for obtaining such derivatives, utilizing reactions of sulfonated lignin with a selected acid halide—thionyl halide, phosphorus halides, or phosphorus oxyhalides. The intermediate product is then reacted with an amine of choice, either primary, secondary, or tertiary. The shown examples include the usage of triamylamine, N-dodecylamine, and hexylamine [32]. A similar patent describes the manufacturing of the lignin sulfonamide-based surfactants for enhanced oil recovery, where spent sulfite liquor, lignosulfonate, or Kraft lignin was reacted with primary amine-containing from 16 to 22 carbon atoms [33]. Another approach to obtain nitrogen-containing lignin derivatives, such as lignin amides, includes the oxidation of lignin with oxygen, air, ozone, peroxides, halogen oxides, permanganates, or metal oxides, to name a few; then, after the introduction of carboxylic groups into the lignin, the reaction with the chosen aryl or alkyl primary or secondary amines follows, yielding the amine derivative of lignin [34]. A similar approach was proposed in the US4786720 and US4859362 patents, where Kraft lignin was modified to increase carboxylic group content by oxidation, the reaction of lignin with maleic anhydride or fumaric acid according to the Diels–Alder mechanism, or by the reaction of phenolic hydroxyls with chloroacetic acid under alkaline conditions. Under non-aqueous conditions, carboxylic groups introduced to lignin may react with polyalkeneamines, such as diethylenetriamine, to yield amidoamines or imidazolines. The described procedure is aimed at obtaining surfactants for tertiary oil recovery or drilling muds [35,36].

Since low-molecular-weight sulfonamides are well-known for their anti-microbial and bacteriostatic properties [37], the introduction of the sulfonamide groups to the lignin may enhance the intrinsic antibacterial properties of lignin. Application of the described method for lignosulfonate modification may enhance other properties of the material, such as its thermal stability.

2. Materials and Methods

2.1. Materials

Sodium lignosulfonate (STARLIG®Na98S, industrial grade) in the form of loose yellow powder was kindly supplied by Lignostar International BV (Hague, The Netherlands). Hydrochloric acid (35–38 wt%) was purchased from Chempur (Piekary Śląskie, Poland), whereas chloroform, chlorosulfonic acid, sodium hydroxide, and dihexylamine were purchased from Sigma-Aldrich (Darmstadt, Germany). All of the chemicals were of analytical grade and used as received.

2.2. Chemical Modification of Sodium Lignosulfonate

A total of 200 g of sodium lignosulfonate (ligS), dried at 90 °C for 24 h under vacuum conditions, was put into a round-bottom flask, and then 500 mL of 2 M hydrochloric acid (HCl) solution was introduced into the vessel. The mixture was heated to 95 °C and reacted for 4 h. After cooling down the contents of the flask to room temperature, the mixture was concentrated using a rotary evaporator at 90 °C, rotated with 50 rpm under the pressure of 200 mBar until the desired degree of evaporation. The resultant sludge was further dehydrated in a desiccator over magnesium sulfate at room temperature. The product was dried under ambient conditions until constant mass and ground using porcelain mortar.

As-prepared lignosulfonic acid (ligH) was subjected to a two-step procedure resulting in the formation of the sulfonamide derivative of lignin. In the first stage, 44.6 g of lignosulfonic

acid (HSO_3Cl) along with 630 cm^3 of chloroform ($CHCl_3$) was placed in a 2 L round-bottom flask equipped with a condenser, submerged in cold water. Then, 18.2 cm^3 of chlorosulfonic acid was added in small quantities while keeping the temperature below 50 °C. After the addition of chlorosulfonic acid, the temperature was kept at 50 °C, and the reaction was carried out for 5 h. The contents of the flask were cooled down to room temperature and then concentrated using the rotary evaporator at 50 °C, rotated at 50 rpm under the pressure of 500 mBar. The resultant sludge containing lignosulfonyl chloride was dried at 60 °C until constant mass.

In the second stage, 20 cm^3 of 10 wt% solution of sodium hydroxide (NaOH) and 80 cm^3 of distilled water were introduced into a 250 mL round flask with a flat bottom. Then, 10 g of dihexylamine (DHA) was added to the mixture and stirred. Finally, 20 g of lignosulfonyl chloride was placed in the flask, and the contents were stirred vigorously for 5 min, then heated to 30 °C with continued stirring. After 15 min, the contents of the flask were cooled down to room temperature, and a solid product was formed. The residue was filtered and washed thoroughly with distilled water and dried in ambient conditions, followed by another filtration with hot water.

The description of the investigated samples is presented in Table 1.

Table 1. Details of the obtained samples.

Sample	Description
ligS	Pure sodium lignosulfonate
ligH	Lignosulfonic acid, obtained via reaction of ligS with HCl
ligH-HSO$_3$Cl	Lignosulfonyl chloride, a product of the reaction of ligH with HSO$_3$Cl
ligH-HSO$_3$Cl-DHA	The main product, sulfonamide derivative of lignin, formed in the reaction of the lignosulfonyl chloride with dihexylamine
ligH-HSO$_3$CL-DHA-HW	The main product after the additional washing with hot distilled water

The schematic route of synthesis is presented in Figure 2.

2.3. Fourier Transform Infrared (FTIR) Spectroscopy

Fourier transform infrared (FTIR) spectra were obtained using a Nicolet iS5 spectrometer (Thermo Fisher Scientific, Waltham, MA, USA) equipped with an ATR iD7 accessory with the diamond crystal. The measurement range was between 4000 and 400 cm^{-1}.

2.4. Solid-State Nuclear Magnetic Resonance (SS-NMR)

Solid-State Nuclear Magnetic Resonance ^{13}C spectrum was recorded using NMR Bruker Avance III 500 MHz spectrometer (Bruker Corporation, Billerica, MA, USA), equipped with a 4 mm probe. The rotation frequency was 8 kHz, whereas resonance frequencies were 128.5 and 500.1 MHz. Contact time was 2 ms, and the number of scans was 512. Chemical shifts were calculated using tetramethylsilane (TMS) as a standard. The Solid-State approach was chosen due to the insolubility of the samples in the typical solvents used in the liquid-state NMR analyses.

2.5. Wide-Angle X-ray Diffraction (WAXD)

Diffractograms of the obtained materials were acquired using a Bruker D2 Phaser (Bruker Corporation, Billerica, MA, USA) diffractometer at room temperature. The data acquisition range was between 3 and 60° of 2Θ angle with an increment of 0.1°.

2.6. Scanning Electron Microscopy (SEM)

The samples' morphology was examined using a JEOL JSM-6010LA Analytical Scanning Electron Microscope (JEOL Ltd., Tokyo, Japan). Each sample was coated with a 4 nm thick layer of gold prior to measurements, which were carried out at an accelerating voltage of 5 kV and 10 mm working distance.
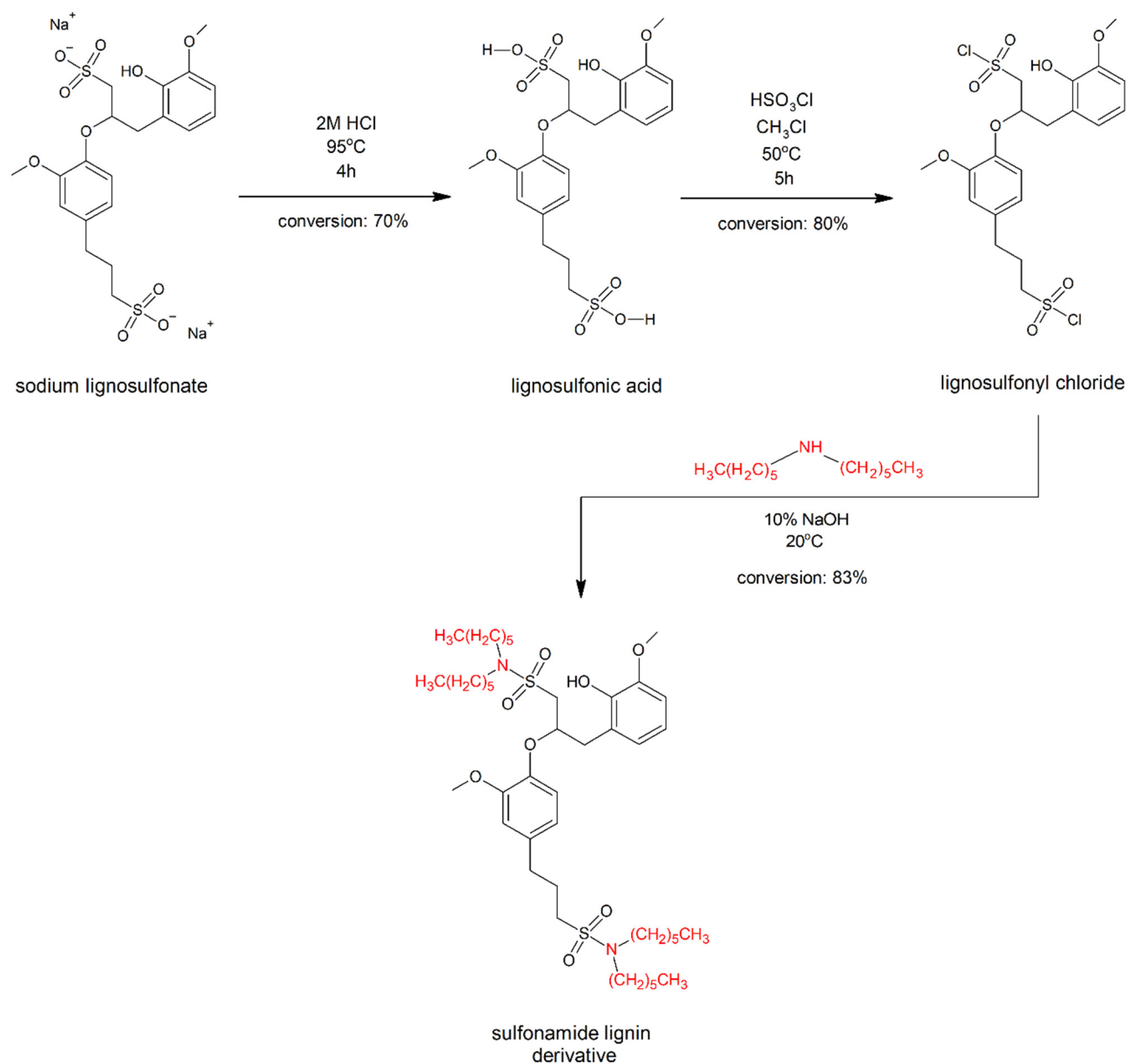
Figure 2. Synthetic route to obtain sulfonamide derivatives of lignin.

2.7. Thermogravimetric Analysis (TGA)

Netzsch TG 209F1 Libra analyzer (Netzsch GmbH, Selb, Germany) was used to carry out the thermogravimetric analysis. Measurements were performed in a temperature range of 30–600 °C, at a heating rate of 10 K/min under oxidative (synthetic air) and inert (argon) atmosphere.

3. Results and Discussion

3.1. FTIR Analysis

Figure 3 presents the FTIR spectra of samples obtained after each stage of the process.
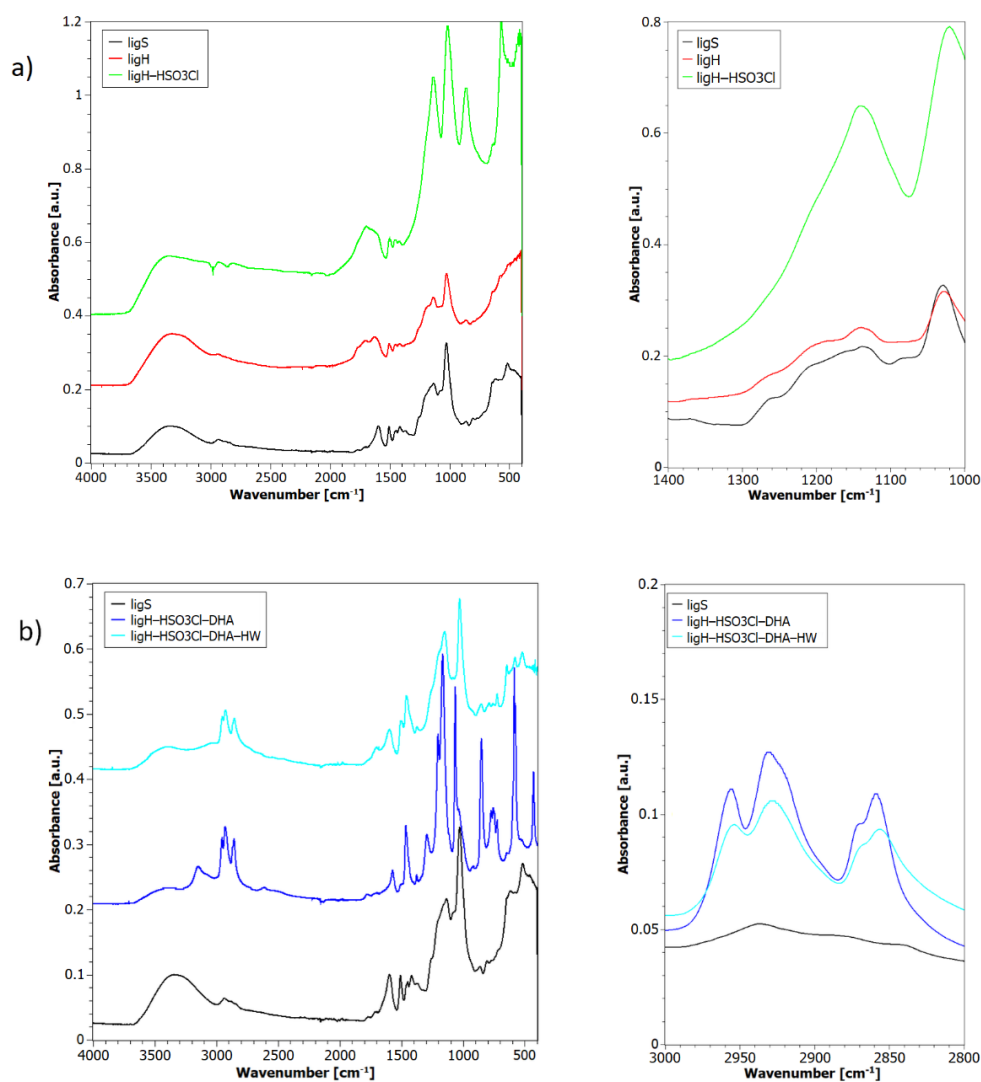
Figure 3. FTIR spectra of the materials obtained after the first (**a**) and the second (**b**) step of the modification procedure.

For the unmodified lignosulfonate (ligS), the broad band present in the spectra at 3340 cm^{-1} is associated with the stretching of the O-H bond in the hydroxyl group. Small bands observed at 2935 and 2880 cm^{-1} correspond with stretching vibrations of the C-H bond of the methyl and methylene groups present in the side chains of the lignosulfonate. At 1600, 1510, and 1420 cm^{-1}, bands corresponding to the stretching of the C=C bond of the backbone vibrations of the aromatic ring are observed. Small bands present at 1450 and 1370 cm^{-1} are connected to symmetric and asymmetric bending of the C-H bond of the methyl group and scissoring vibrations of the C-H bond in the methylene group. At 1340 cm^{-1}, there is a visible band, characteristic of phenols, which originates from the stretching of the C-O bond. The next band visible on the spectrum consists of the overlapping bands originating from the asymmetric stretching vibrations of the C-O-C bond, characteristic of ethers at 1137 cm^{-1}, as well as asymmetric and symmetric stretching of the -SO$_2$- group at 1160 and 1200 cm^{-1}. A single, strong band at 1029 cm^{-1} is the result of the stretching of C-O, characteristic of the primary alcohols. Moreover, the absorption band visible for 652 cm^{-1} is typical for the lignosulfonates and is the result of the vibrations of the S-O bond [38,39]. The spectrum obtained for the lignosulfonic acid (ligH) does not exhibit significant differences from the ligS spectrum.

As for the material modified with the chlorinating agent, to observe the effect of the reaction, it is necessary to follow the changes in the bands connected with the sulphonyl group. As presented in Figure 3a, bands visible at 1200, 1140, and 1020 cm^{-1} associated with the asymmetric and symmetric stretching of the -SO$_2$- group can be observed for all of the samples. For the sample obtained after the reaction with the chlorinating agent (ligH-HSO$_3$Cl), the intensity of the bands is significantly greater than for those of the reference samples (ligS and ligH).

For the final lignin-based material modified with dihexylamine, new bands of medium intensity, located at 3000–2800 cm^{-1}, associated with the vibrations of the methyl and methylene groups present in the alkyl chains of dihexylamine, appear. The bands visible at 2960 and 2870 cm^{-1} as well as 2935 and 2850 cm^{-1} originate from the asymmetric and symmetric stretching of the C-H bond present in the methyl and methylene groups, respectively. Other relevant bands, characteristic for the sulfonamides, are present in the sulphonyl range—weak bands at 1380–1320 cm^{-1} are connected with the asymmetric stretching of the -SO$_2$- group, whereas bands at 1200–1140 cm^{-1} are characteristic for the symmetric vibrations. At 950–860 cm^{-1}, weak bands present in the spectra correspond to the stretching of the N-S bond of the sulfonamide.

3.2. Solid-State Nuclear Magnetic Resonance

The final sample obtained in the modification process, ligH-HSO$_3$Cl-DHA-HW, was subjected to analysis via ^{13}C SS-NMR spectroscopy (Figure 4). The peaks present in the spectrum between 14.4 and 50 ppm are related to the carbon atoms of the hexyl chains originating from dihexylamine. The carbon atoms farthest located from the nitrogen atom give a peak at 14.4 ppm chemical shift; the next observable peaks are at 23 ppm and 26.6 ppm, 31.8 ppm, and the last one, 49 ppm, which corresponds to the carbon atoms closest to the nitrogen. The dihexylamine part should give six peaks, but due to the proximity of the chemical shifts (three peaks between 27 and 33 ppm), only two are visible on the spectrum (Figure 4) because of the overlapping. The peak at 56 ppm may be associated with carbons of the methoxyl group present in lignins. As for the broad, irregularly shaped peaks between 100 and 160 ppm, signals from 100 to 120 ppm correspond to the carbons from the -CH- groups of alkyl chains present in the intrinsic structure of the lignosulfonate, whereas those between 120 and 160 ppm are related to the aromatic carbon atoms. Due to the overlapping of the peaks, it is difficult to distinguish between the specific signals, although there is a clear maximum at 147 ppm [40].

Although in recent years, the analysis of the native lignins by means of NMR has seen significant progress, there are only a few reports concerning the NMR study of the lignosulfonates [41]. Lutnaes et al. proposed a ^{1}H and ^{13}C NMR investigation of 15 model compounds of the various structures present in the lignosulfonate, and the presented results are consistent with their findings [42].

3.3. WAXD Analysis

WAXD diffractograms obtained for the raw material, reference sample, as well as modified lignins are shown in Figure 5.

The diffractograms reveal that all of the obtained samples display amorphous structure, represented by the broad, amorphous halo between 7 and 30° of the 2Θ angle. The sharp crystalline peak with high intensity, observed for the 32° and a smaller peak at 45°, present in the diffraction pattern of the ligH sample, can be associated with sodium chloride [43], which is formed as a by-product of the hydrolysis reaction. For the ligH-HSO$_3$Cl-DHA sample, there is a small, narrow peak at 7° of the 2Θ angle, probably caused by the water-soluble impurities, which were removed by the washing of the sample with hot distilled water (ligH-HSO$_3$Cl-DHA-HW). This remains coherent with the earlier research, which confirmed the amorphous, highly disorganized structure of lignin [7].
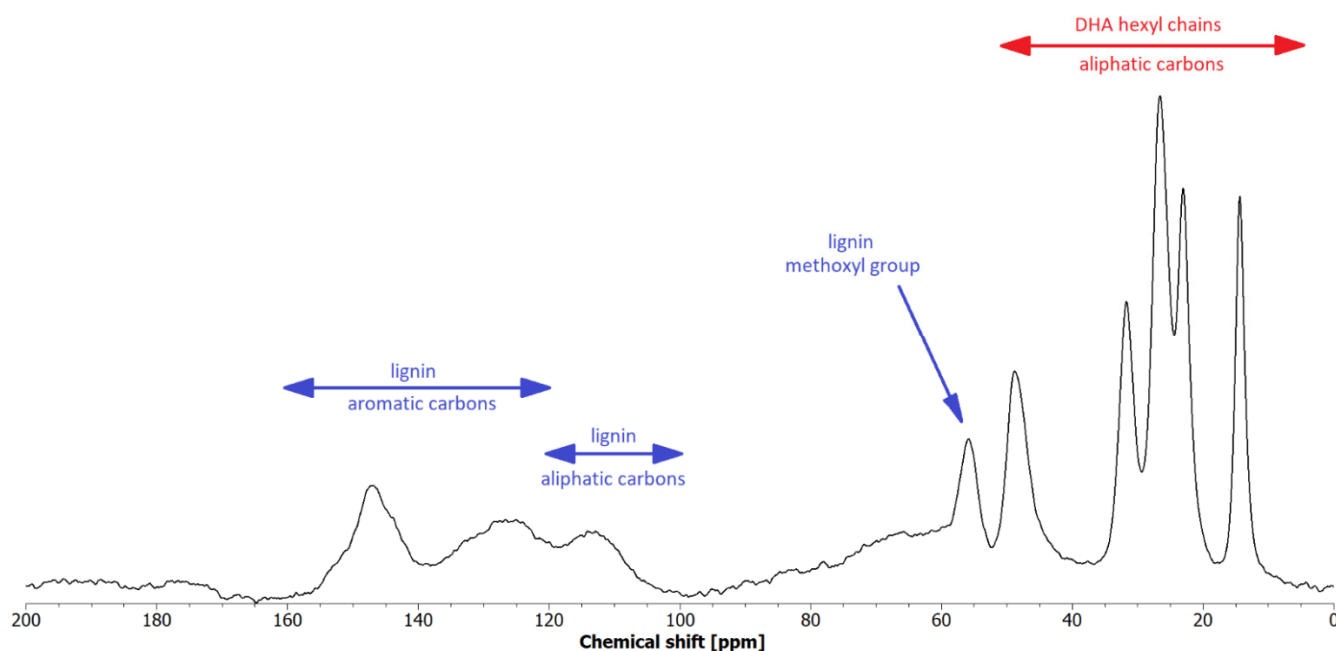
Figure 4. Solid-State ^{13}C NMR spectrum of the ligH-HSO$_3$Cl-DHA-HW sample.
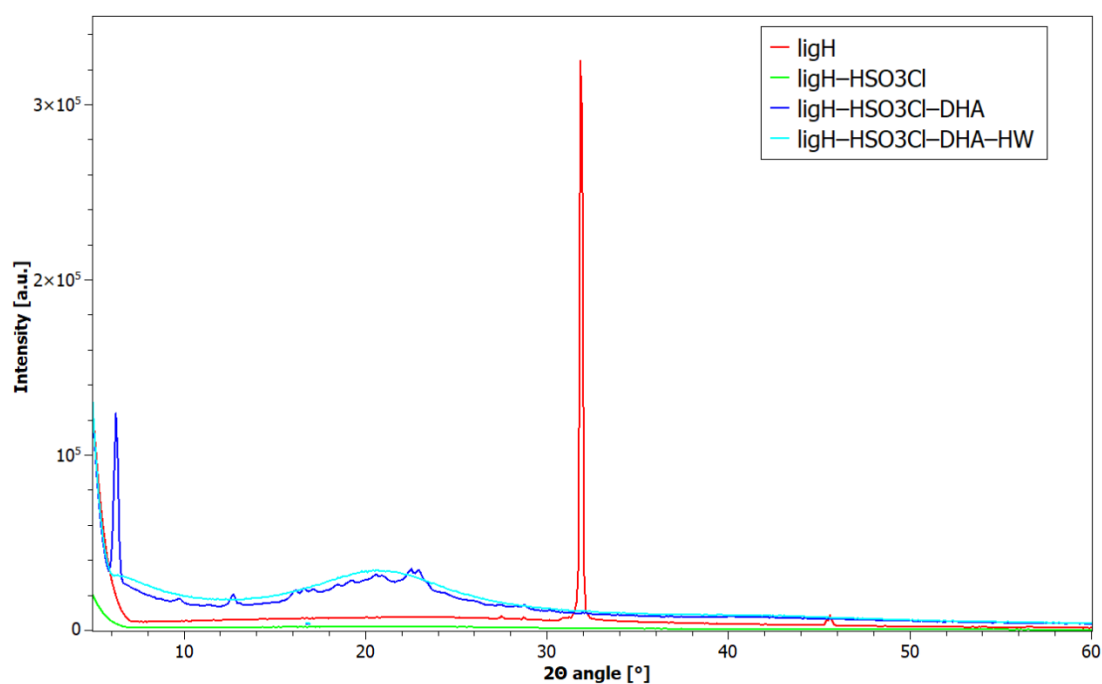

Figure 5. Diffraction patterns of the investigated materials.

3.4. SEM Analysis

Morphology of the obtained materials was assessed by analysis of the SEM micropho-tographs of the samples' surface (Figure 6). Material obtained after the acidic hydrolysis of the sodium lignosulfonate (ligH) displays an irregular, porous, layered structure, as well as sporadically occurring structures with regular, cubic shapes. This observation, along with the results of the WAXD analysis, indicates the presence of crystallized sodium chloride, which was not removed during the preparation of the samples. For ligH-HSO$_3$Cl, the layered structure of the material was also observed, though the platelets building the layers were not so pronounced. Occasional pores of a few micrometers in diameter were also

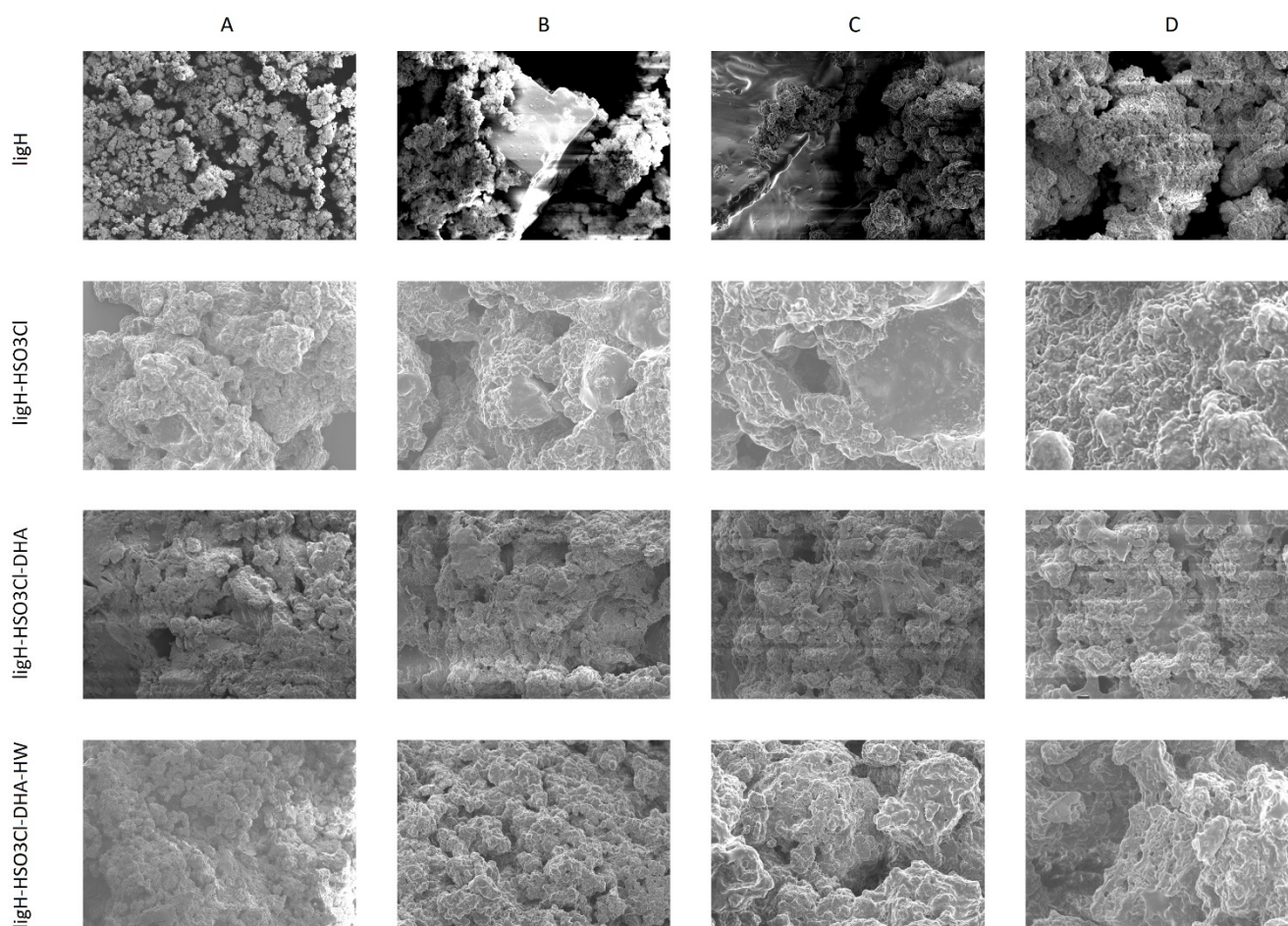visible. The morphology of the ligH-HSO$_3$Cl-DHA and ligH-HSO$_3$Cl-DHA-HW did not exhibit significant changes.

Figure 6. Morphology of the lignins obtained after both steps of the modification procedure: Column (**A**) magnification 200×, (**B**) 500×, (**C**) 1000×, (**D**) 2000×. Imaging conditions were described in Section 2.6.

3.5. TGA Analysis

Thermogravimetric data were obtained for the temperatures ranging from 30 to 600 °C. Figure 6 presents TG and DTG curves obtained in both synthetic air and argon atmosphere for the reference samples as well as those subjected to modification with DHA.

As seen in Figure 7a, all of the samples exhibit slightly different thermo-oxidative decomposition behavior, though three stages of thermal degradation can be observed for all of the examined samples. Both ligS and ligH materials exhibit about 5% weight loss below 200 °C, which may be attributed to the removal of the residual moisture from the material. Those two lignins exhibit a similar degradation profile up to 400 °C. Above this temperature, ligS does not change its weight significantly, leaving about 50% of the initial mass as the char residue. LigH loses more of its mass, with the residue at 600 °C making up 25% of the initial mass. LigH-HSO$_3$Cl displays the worst thermal stability due to mass loss below 200 °C being almost 40% of the initial mass.
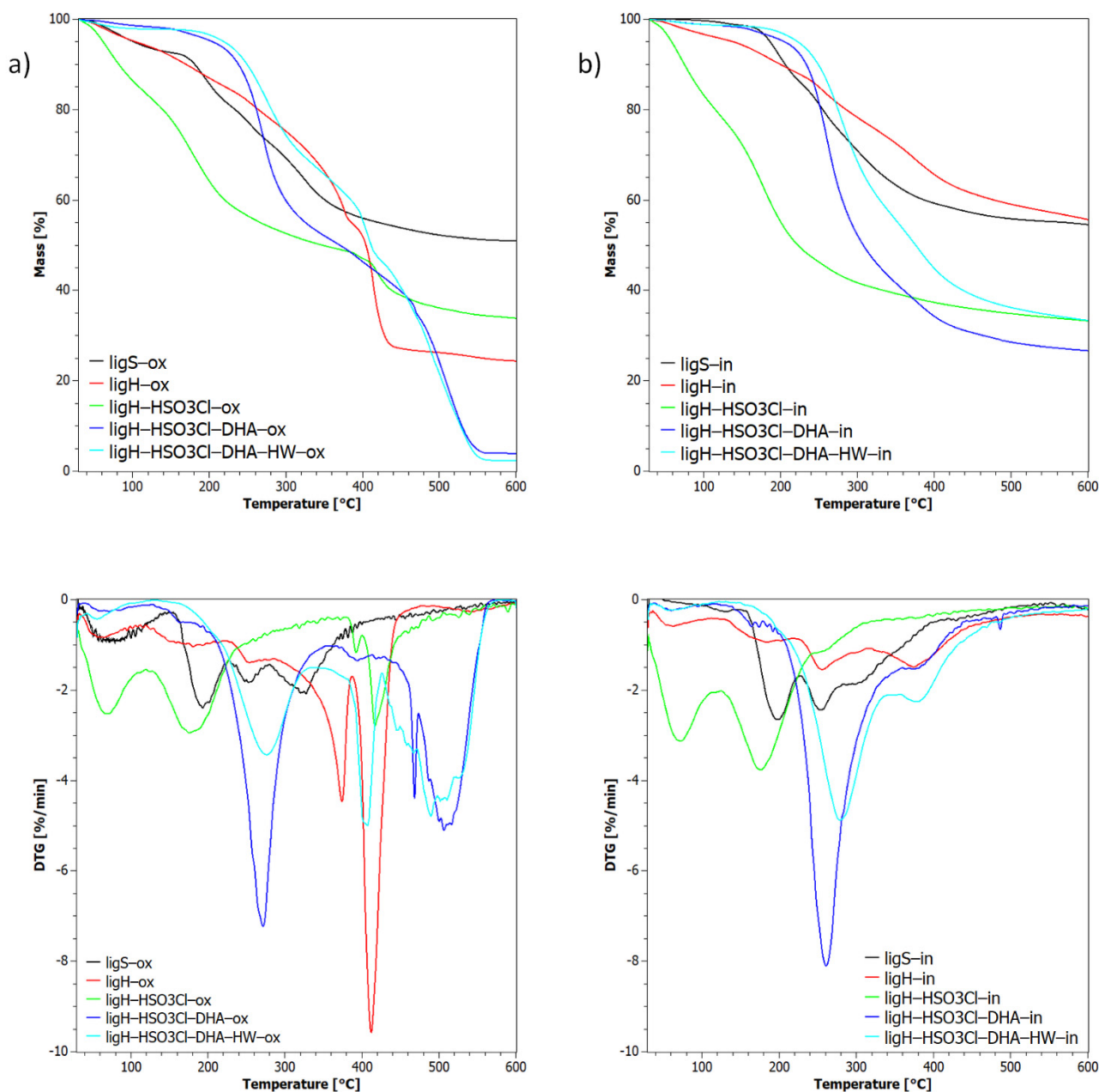
Figure 7. TG and DTG curves of the investigated materials during thermo-oxidative (**a**) and pyrolitic (**b**) degradation.

For the pyrolytic degradation shown in Figure 7b, a similar trend can be observed. ligH-HSO$_3$Cl exhibits the worst thermal properties, whereas ligH-HSO$_3$Cl-DHA and ligH-HSO$_3$Cl-DHA-HW display improved thermal behavior. This observation is consistent with the results obtained for thermo-oxidative degradation, where ligH-HSO$_3$Cl-DHA-HW was characterized by the highest temperatures of the thermal-degradation parameters, as presented in Table 2. Most of the tested materials, apart from ligH-HSO$_3$Cl, show an increased char residue at 600 °C in relation to measurements carried out in the synthetic air atmosphere. The shape of the profiles above 500 °C suggests a possibility of the ongoing pyrolytic degradation process, which indicates the need to re-run the measurements at a wider temperature range.

Table 2. Parameters of the thermal decomposition of the lignin-based materials.

Material	Degradation in Synthetic Air				Degradation in Argon			
	$T_{5\%}$ (°C)	$T_{20\%}$ (°C)	T_{max} (°C)	Char Residue at 600 °C (%)	$T_{5\%}$ (°C)	$T_{20\%}$ (°C)	T_{max} (°C)	Char Residue at 600 °C (%)
ligS	101	234	193	50.9	187	255	199	52.0
ligH	104	264	412	24.4	139	285	374	55.5
ligH-HSO$_3$Cl	62	139	392	33.8	58	115	176	33.1
ligH-HSO$_3$Cl-DHA	205	261	272	3.9	205	252	261	26.6
ligH-HSO$_3$Cl-DHA-HW	219	281	407	2.2	223	275	279	33.3

The improvement of thermal properties observed for the samples modified with DHA may be associated with the blocking of the sulfonyl group due to its reaction with the diamine. It is known that in the case of cellulosic materials containing sulfonyl groups on their surface, i.e., cellulose nanocrystals obtained via acidic hydrolysis utilizing sulfuric acid, sulfonyl groups cause the deterioration of thermal properties [44]. The formation of the sulfonamide group may have a blocking effect on the sulfonyl group, preventing the desulfonation and consecutive deterioration of the thermal properties.

Taking into account the parameters characterizing the thermal-degradation process presented in Table 2, it is possible to incorporate as-prepared sulfonamide lignin derivatives into thermoplastic matrices with melting temperatures by ca. 200 °C, especially biopolymers, to obtain 'all-green' biocomposites.

4. Conclusions

In our work, sodium lignosulfonate was modified via a two-step chemical route using chlorosulfonic acid and dihexylamine to yield a sulfonamide derivative of lignin. FTIR results confirm the presence of the alkyl chains and the formation of the bond between sulfur and nitrogen in the sulfonyl group. No structural changes occurred during the modification procedure, as evidenced by WAXD analysis. Thermal stability of the modified lignin is considerably improved in relation to the raw materials, especially when looking at changes of the T5% temperature—the final modified material showed an improvement of the said parameter of 115 °C in comparison with the raw material (219 °C vs. 104 °C, respectively). Moreover, fewer charred residues are present at 600 °C, which may be caused by the change in the thermal degradation mechanism owing to the introduction of the nitrogen-based compounds into the structure of the investigated lignin derivatives. The formation of the sulfonamide may retard the desulfonation, which in turn enables the improvement of the thermal-degradation parameters. SS-NMR confirmed the incorporation of dihexylamine to the lignosulfonate structure and the formation of the dialkyl sulfonamide derivative. The described method of the chemical modification of lignosulfonates with secondary amines has the potential for obtaining functional, lignin-based materials that can be used as a value-added filler for polymer composites with biopolymer matrices. Further studies focusing on utilizing different types of secondary amines to obtain sulfonamide derivatives of lignin are currently underway.

Author Contributions: Conceptualization, K.K. and T.M.M.; methodology, K.K., T.M.M. and K.P.; software, K.K.; validation, K.K., T.M.M. and K.P.; formal analysis, K.K. and T.M.M.; investigation, K.K. and T.M.M.; resources, K.P.; data curation, K.K.; writing—original draft preparation, K.K.; writing—review and editing, K.P.; visualization, K.K.; supervision, K.P.; project administration, T.M.M. and K.P. All authors have read and agreed to the published version of the manuscript.

Institutional Review Board Statement: Not applicable.

Informed Consent Statement: Not applicable.

References

1. Faris, A.H.; Rahim, A.A.; Mohamad Ibrahim, M.N.; Hussin, M.H.; Alkurdi, A.M.; Salehabadi, A. Investigation of oil palm based Kraft and auto-catalyzed organosolv lignin susceptibility as green wood adhesives. *Int. J. Adhes. Adhes.* **2017**, *74*, 115–122. [CrossRef]
2. Calvo-Flores, F.G.; Dobado, J.A. Lignin as renewable raw material. *ChemSusChem* **2010**, *3*, 1227–1235. [CrossRef] [PubMed]
3. Xu, F.; Yu, J.; Tesso, T.; Dowell, F.; Wang, D. Qualitative and quantitative analysis of lignocellulosic biomass using infrared techniques: A mini-review. *Appl. Energy* **2013**, *104*, 801–809. [CrossRef]
4. Gellerstedt, G.; Henriksson, G. Lignins: Major Sources, Structure and Properties. In *Monomers, Polymers and Composites from Renewable Resources*, 1st ed.; Belgacem, M.N., Gandini, A., Eds.; Elsevier: Amsterdam, The Netherlands, 2008; pp. 201–224.
5. Beisl, S.; Friedl, A.; Miltner, A. Lignin from micro- to nanosize: Applications. *Int. J. Mol. Sci.* **2017**, *18*, 2367. [CrossRef] [PubMed]
6. Doherty, W.O.S.; Mousavioun, P.; Fellows, C.M. Value-adding to cellulosic ethanol: Lignin polymers. *Ind. Crops Prod.* **2011**, *33*, 259–276. [CrossRef]
7. Brauns, F.E.; Brauns, D.A. *The Chemistry of Lignin. Supplement Volume Covering the Literature 1949–1958*, 1st ed.; Academic Press Inc.: London, UK, 1960.
8. Liao, J.J.; Latif, N.H.A.; Trache, D.; Brosse, N.; Hussin, M.H. Current advancement on the isolation, characterization and application of lignin. *Int. J. Biol. Macromol.* **2020**, *162*, 985–1024. [CrossRef]
9. Arapova, O.V.; Chistyakov, A.V.; Tsodikov, M.V.; Moiseev, I.I. Lignin as a Renewable Resource of Hydrocarbon Products and Energy Carriers (A Review). *Pet. Chem.* **2020**, *60*, 227–243. [CrossRef]
10. Duval, A.; Lawoko, M. A review on lignin-based polymeric, micro- and nano-structured materials. *React. Funct. Polym.* **2014**, *85*, 78–96. [CrossRef]
11. Nord, F.F.; Schubert, W.J. Lignin. *Sci. Am.* **1958**, *199*, 104–113. [CrossRef]
12. Aro, T.; Fatehi, P. Production and Application of Lignosulfonates and Sulfonated Lignin. *ChemSusChem* **2017**, *10*, 1861–1877. [CrossRef]
13. Figueiredo, P.; Lintinen, K.; Hirvonen, J.T.; Kostiainen, M.A.; Santos, H.A. Properties and chemical modifications of lignin: Towards lignin-based nanomaterials for biomedical applications. *Prog. Mater. Sci.* **2018**, *93*, 233–269. [CrossRef]
14. Laurichesse, S.; Avérous, L. Chemical modification of lignins: Towards biobased polymers. *Prog. Polym. Sci.* **2014**, *39*, 1266–1290. [CrossRef]
15. Ninz, H. *Wood Adhesives: Chemistry and Technology*, 1st ed.; Pizzi, A., Ed.; Marcel Dekker: New York, NY, USA, 1983; pp. 247–288.
16. Karimov, O.K.; Teptereva, G.A.; Chetvertneva, I.A.; Movsumzade, E.M.; Karimov, E.K. The structure of lignosulfonates for production of carbon catalyst support. *IOP Conf. Ser. Earth Environ. Sci.* **2021**, *839*, 022086. [CrossRef]
17. Henn, A.; Mattinen, M.L. Chemo-enzymatically prepared lignin nanoparticles for value-added applications. *World J. Microbiol. Biotechnol.* **2019**, *35*, 125. [CrossRef]
18. Chen, K.; Yuan, S.; Wang, D.; Liu, Y.; Chen, F.; Qi, D. Basic Amino Acid-Modified Lignin-Based Biomass Adjuvants: Synthesis, Emulsifying Activity, Ultraviolet Protection, and Controlled Release of Avermectin. *Langmuir* **2021**, *37*, 12179–12187. [CrossRef]
19. Pradhan, S.K.; Chakraborty, I.; Kar, B.B. Chemically Modified Lignin—A Potential Resource Material for Composites with Better Stability. *Int. J. Sci. Environ. Technol.* **2015**, *4*, 183–189.
20. Cateto, C.A.; Barreiro, M.F.; Rodrigues, A.E.; Belgacem, M.N. Optimization study of lignin oxypropylation in view of the preparation of polyurethane rigid foams. *Ind. Eng. Chem. Res.* **2009**, *48*, 2583–2589. [CrossRef]
21. Chen, K.; Lei, L.; Lou, H.; Niu, J.; Yang, D.; Qiu, X.; Qian, Y. High internal phase emulsions stabilized with carboxymethylated lignin for encapsulation and protection of environmental sensitive natural extract. *Int. J. Biol.* **2020**, *158*, 430–442. [CrossRef]
22. Malutan, T.; Nicu, R.; Popa, V.I. Lignin modification by epoxidation. *BioResources* **2008**, *3*, 1371–1376.
23. Brežny, R.; Paszner, L.; Micko, M.M.; Uhrín, D. The Ion-Exchanging Lignin Derivatives Prepared by Mannich Reaction with Amino Acids. *Holzforschung* **1988**, *42*, 369–373. [CrossRef]
24. Kazzaz, A.E.; Feizi, Z.H.; Fatehi, P. Grafting strategies for hydroxy groups of lignin for producing materials. *Green Chem.* **2019**, *21*, 5714–5752. [CrossRef]
25. Matsushita, Y. Conversion of technical lignins to functional materials with retained polymeric properties. *J. Wood. Sci.* **2015**, *61*, 230–250. [CrossRef]
26. Jiang, C.; Bo, J.; Xiao, X.; Zhang, S.; Wang, Z.; Yan, G.; Wu, Y.; Wong, C.; He, H. Converting waste lignin into nano-biochar as a renewable substitute of carbon black for reinforcing styrene-butadiene rubber. *Waste Manag.* **2020**, *102*, 732–742. [CrossRef] [PubMed]

27. Wu, Y.; Qian, Y.; Zhang, A.; Lou, H.; Yang, D.; Qiu, X. Light color dihydroxybenzophenone grafted lignin with high UVS/UVB absorbance ratio for efficient and safe natural sunscreen. *Ind. Eng. Chem. Res.* **2020**, *59*, 17037–17068. [CrossRef]

28. Dai, K.; Zhao, G.; Wang, Z.; Peng, X.; Wu, J.; Yang, P.; Li, M.; Tang, C.; Zhuang, W.; Ying, H. Novel Mesoporous Lignin-Calcium for Efficiently Scavenging Cationic Dyes from Dyestuff Effluent. *ACS Omega* **2021**, *6*, 816–826. [CrossRef]

29. Gao, B.; Chang, Q.; Yang, H. Selective absorption of ofloxacin and ciprofloxacin from a binary system using lignin-based absorbents: Quantitative analysis, adsorption mechanisms, and structure-activity relationships. *Sci. Total* **2021**, *765*, 144427. [CrossRef]

30. Ji, X.; Guo, M.; Zhu, I.; Du, W.; Wang, H. Synthesis Mechanism of an Environment-Friendly Sodium Lignosulfonate/Chitosan Medium-Density Fiberboard Adhesive and Response Bonding Performance to Synthesis Mechanism. *Materials* **2020**, *13*, 5697. [CrossRef]

31. Qian, Y.; Zhou, Y.; Lu, M.; Guo, X.; Yang, D.; Lou, H.; Qiu, X.; Guo, C.F. Direct Construction of Catechol Lignin for Engineering Long-Activity Conductive, Adhesive and UV-Blocking Hydrogel Bioelectronics. *Small Methods* **2021**, *5*, e2001311. [CrossRef]

32. Kim, C.S.Y. Lignosulfonamide and a Process for Its Preparation. U.S. Patent 3,438,960, 15 April 1969.

33. DeBons, F.E.; Whittington, L.E.; Pedersen, L.D. Method of Enhanced Oil Recovery and Compositions Useful Therein. U.S. Patent 4,548,721, 22 October 1985.

34. Kim, C.S.Y. Nitrogen and Lignin Containing Products and Process for Obtaining Them. U.S. Patent 3,538,071, 3 November 1970.

35. Schilling, P. Sulfomethylated Lignin Amines. U.S. Patent 4,786,720, 22 November 1988.

36. Schilling, P. Sulfomethylated Lignin Amines. U.S. Patent 4,859,362, 22 August 1989.

37. Vinagreiro, C.S.; Gonçalves, N.P.F.; Calvete, M.J.F.; Schaberle, F.A.; Arnaut, L.G.; Pereira, M.M. Synthesis and characterization of biocompatible bimodal meso-sulfonamide-perfluorophenylporphyrins. *J. Fluor. Chem.* **2015**, *180*, 161–167. [CrossRef]

38. Zhou, H.; Shi, X.; Wu, W.; An, X.; Tian, Y.; Qiao, Y. Facile preparation of lignosulfonate/N-methylaniline composite and its application in efficient removal of Cr(VI) from aqueous solutions. *Int. J. Biol. Macromol.* **2020**, *154*, 1194–1204. [CrossRef]

39. Jiang, C.; He, H.; Yao, X.; Yu, P.; Zhou, L.; Jia, D. The aggregation structure regulation of lignin by chemical modification and its effect on the property of lignin/styrene–butadiene rubber composites. *J. Appl. Polym. Sci.* **2018**, *135*, 45759. [CrossRef]

40. Gil, A.M.; Neto, C.P. Solid-State Nmr Studies of Wood And Other Lignocellulosic Materials. In *Annual Reports on NMR Spectroscopy*, 1st ed.; Webb, G.A., Ed.; Academic Press: Cambridge, MA, USA, 1999; Volume 37, pp. 75–117.

41. Brudin, S.; Schoenmakers, P. Analytical methodology for sulfonated lignins. *J. Sep. Sci.* **2010**, *33*, 439–452. [CrossRef] [PubMed]

42. Lutnaes, B.F.; Myrvold, B.O.; Lauten, R.A.; Endeshaw, M.M. 1H and 13C NMR data of benzylsulfonic acids—Model compounds for lignosulfonate. *Magn. Reson. Chem.* **2008**, *46*, 299–305. [CrossRef] [PubMed]

43. Addala, S.; Bouhdjer, L.; Chala, A.; Bouhdjar, A.; Halimi, O.; Boudine, B.; Sebais, M. Structural and optical properties of a NaCl single crystal doped with CuO nanocrystals. *Chinese Phys. B* **2013**, *22*, 098103. [CrossRef]

44. Roman, M.; Winter, W.T. Effect of sulfate groups from sulfuric acid hydrolysis on the thermal degradation behavior of bacterial cellulose. *Biomacromolecules* **2004**, *5*, 1671–1677. [CrossRef]